

CORAL8: Concurrent Object Regression for Area Localization in Medical Image Panels

Sam Maksoud*, Arnold Wiliem, Kun Zhao, Teng Zhang,
Lin Wu and Brian C. Lovell

The University of Queensland, School of ITEE, QLD 4072, Australia

June 25, 2019

Abstract

This work tackles the problem of generating a medical report for multi-image panels. We apply our solution to the Renal Direct Immunofluorescence (RDIF) assay which requires a pathologist to generate a report based on observations across the eight different WSI in concert with existing clinical features. To this end, we propose a novel attention-based multi-modal generative recurrent neural network (RNN) architecture capable of dynamically sampling image data concurrently across the RDIF panel. The proposed methodology incorporates text from the clinical notes of the requesting physician to regulate the output of the network to align with the overall clinical context. In addition, we found the importance of regularizing the attention weights for word generation processes. This is because the system can ignore the attention mechanism by assigning equal weights for all members. Thus, we propose two regularizations which force the system to utilize the attention mechanism. Experiments on our novel collection of RDIF WSIs provided by a large clinical laboratory demonstrate that our framework offers significant improvements over existing methods.

1 Introduction

Automatic image captioning [17] is an important topic in the medical research area as it frees pathologists from manual medical image interpretation and reduces the cost significantly [6]. Typically this involves conditioning a recurrent neural network (RNN) on image features encoded by a convolutional neural network (CNN). This method has shown great promise in non-specific image captioning tasks but has not generalized well to the complex domain of medical images [18, 19].

A common solution is to employ a pathologist to annotate training data [19]. However,

*s.maksoud@uqconnect.uq.edu.au; arnold.wiliem@ieee.org;
{k.zhao1, t.zhang, lin.wu} @uq.edu.au; lovell@itee.uq.edu.au

even with access to annotated image features and medical reports, the overall clinical context is still important in medical image interpretation. This is because certain pathologies may be morphologically indistinguishable. One such case is the differential diagnoses of immunotactoid glomerulonephritis and diabetic nephropathy. In the Renal Direct Immunofluorescence (RDIF) assay, both conditions can present with linear accentuation of the glomerular basement membrane for IgG; the significance of this pattern cannot be determined without clinical confirmation/exclusion of diabetes mellitus [1]. For this reason, image captioning models conditioned solely on image data may not be the ideal solution for tasks in the medical domain.

The second major challenge of image captioning task in medical domain is correlating information from multiple images. For example, a pathologist must interpret a set of 8 different renal biopsy sections of the same patient to report the RDIF assay. Several methods have been proposed to enable captioning of multiple images by assuming images in the set exhibit temporal dependence [4] or contain multiple views/instances of the same object [18]. These assumptions are unsuitable for the multi-object temporally independent RDIF set. We refer to this problem as the ordered set to sequence problem: it must be an ordered set to preserve the identity of the antibody in the RDIF panel.

To address the problems outlined above, we describe a novel framework to overcome the clinical context bias and generate a RDIF medical report. The contributions of this paper are listed as follows:

1. To our knowledge, we are the first work to solve the ordered set to sequence problem by proposing a novel attention based architecture which provides concurrent access to all images at each step and models the clinical notes as priors to regulate clinical contexts.
2. We also introduce two novel regulators, Salient Alpha (SAL) and Time Distributed Variance (TDVAR), to discourage uniform attention weights.
3. Finally, we will release a novel RDIF dataset¹ with quantitative baseline results provided using metrics from BLEU [13], ROUGE [11] and METEOR [2].

2 Renal Direct Immunofluorescence Dataset

The novel RDIF dataset used in this paper was assembled from routine clinical samples in collaboration with Sullivan Nicolaides Pathology; a subsidiary of Sonic Healthcare Limited. To prepare the RDIF slides, eight separate sections of renal biopsy tissue are treated with fluorescein isothiocyanate (FITC) conjugated antibodies to one of either IgG, IgA, IgM, Kappa, Lambda, C1q, C3 or Fibrinogen antibodies. The dataset comprises of 144 patient samples split into 99 training, 15 validation and 30 test sets. Each sample contains the eight WSIs, the clinical notes of the requesting physician, and the medical report.

¹<https://github.com/cradleai/rdif>

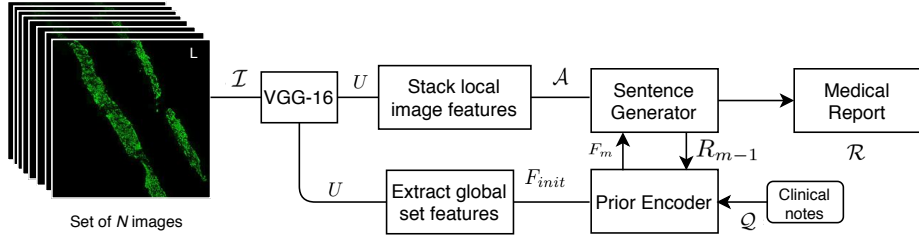


Figure 1: This image illustrates the framework of the proposed CORAL8 Architecture.

3 Proposed Method - CORAL8

3.1 Architecture

As illustrated in Fig. 1, the main aim of CORAL8 is to generate a medical report, \mathcal{R} from an ordered set of images \mathcal{I} and clinical notes \mathcal{Q} . To this end, we train a sentence generator ϕ_s which receives a report context vector and local image features vector as input and generates sequence of words. There are several desirable properties that we enforce in the sentence generator:

1. It must generate coherent sentences;
2. The generated sentences must be in concert with the clinical contexts described in the clinical notes;
3. The attention mechanism must produce diverse representations of local image features for the report generation. The mechanism must also ensure that local features from each image in the set are equally represented in the generative sequence.

To generate coherent sentences, we train a neural network called the prior encoder ϕ_p which extracts context features F_m ; where m is the index of the sentence. The context features are a joint representation of; (1) previous sentence features; and (2) previous context features. To encourage agreement between the generated report and the clinical context, we feed the prior encoder with; (1) clinical notes features and (2) global image set features. This can be interpreted as forming a general impression of the image features with respect to the clinical context. The context features will then be fed into the sentence generator. Finally, to ensure that the model attends to each image in the set, we use a regulated attention mechanism to generate a dynamic local image features conditioning vector L_t used to generate the next word in the sentence. We describe these components in detail below.

Image Encoder encodes an ordered set of images $\mathcal{I} = \{I_1, \dots, I_N\}$ into the set of local image features \mathcal{A} and the global image features F_{init} . More specifically, we first extract the $14 \times 14 \times 512$ features U from the 4th max-pool layer of the pre-trained VGG-16 network [16]. Then the extracted features U are concatenated and flattened to compute

the local image representations, $\mathcal{A} = \{A_1, \dots, A_a\}, A_i \in \mathbb{R}^{N \times d}$ where $a = 196$ and $d = 512$ are the dimensions of the flattened image and feature channels respectively. Meanwhile, in order to produce a global representation for \mathcal{I} , we apply an FC layer to U to extract F_{init} with $1 \times H$ fixed dimensions. Then, \mathcal{A} and F_{init} are fed into the following attention and context encoder networks.

Prior Encoder extracts the context vector F_m to represent features from the clinical notes and previously generated sentence R_{m-1} . More specifically, for each sentence we first use a word embedding to produce fixed vector representations $\mathcal{S} = \{s_1, \dots, s_C\}, s_t \in \mathbb{R}^{V \times E}$ and $\mathcal{Q} = \{q_1, \dots, q_C\}, q_i \in \mathbb{R}^{V \times E}$ for the set of words in the previous sentence and clinical notes respectively; where, V is the size of the vocabulary, C is the number of words in each sentence, $E = 512$ is the word embedding space and q_i and s_t are both 1-of- V encoded words. R_{m-1} is then fed into a bidirectional LSTM [5] and followed by an FC layer to encode a fixed $1 \times H$ representation J_m . We then concatenate J_m and F_{m-1} and apply an FC layer to encode F_m with $1 \times H$ fixed dimensions. At $m = 0$, the output of the image encoder F_{init} and the embed clinical notes \mathcal{Q} are used in place of F_{m-1} and R_{m-1} respectively.

Sentence Generator is an RNN that generates a sentence \hat{R}_m word by word conditioned on the outputs of image encoder \mathcal{A} and prior encoder F_m . After a sentence is generated, the prior encoder receives it as input to generate F_{m+1} which is then fed back to the sentence generator to generate the next sentence: this is repeated until the entire medical report is generated. More specifically, the attention network first computes a probability distribution over \mathcal{A} using the deterministic soft attention methods described in [17] to compute κ_{ti} . κ_{ti} is then used to compute the weighted inter-image features vector $\mathcal{Z}_t = \phi(\{A_i\}, \{\kappa_i\}) = \sum_i^a \kappa_i A_i$. The network then computes a second probability distribution α_{ti} in the same way over $\mathcal{Z}_t = \{z_1, \dots, z_N\}, z_i \in \mathbb{R}^d$. The second soft attention weighted inter-image feature vector $L_t = \phi(\alpha(\{z_i\}, \{\alpha_i\}) = \sum_i^N \alpha_i z_i$ serves as the $1 \times d$ local features conditioning vector used to generate s_{t+1} . L_t and h_t are then passed through to a visual sentinel. The visual sentinel multiplies L_t and F_m by gating scalars β_L and β_F . Both gating scalars; are computed as follows

$$\beta_x = \text{Sigmoid}(w_x h_t + b_x) \quad (1)$$

where w_x and b_x are hyper-parameters to be learned by the network. This allows the network to judge the importance of L_t and F_m features when generating s_{t+1} . $\beta_L L_t$, $\beta_F F_m$ and s_t are concatenated and fed into a LSTM. A deep multilayer perceptron output layer (MLP) [14] then computes $\mathcal{X}_{prob} = \{p_i, \dots, p_V\}$; the probability distribution over the vocabulary of V words using the $1 \times H$ hidden state h_t output of the LSTM. Specifically, MLP takes s_t , L_t , h_t and F_m as input and computes the probability distribution for s_t as:

$$p(S_t | S_{t-1}, L_t, F_m) = \tanh(W_v(S_{t-1} + W_h h_t + W_L L_t + W_F F_m)) \quad (2)$$

Where $W_v \in \mathbb{R}^{V \times E}$, $W_h \in \mathbb{R}^{H \times E}$, $W_L \in \mathbb{R}^{Exd}$, $W_F \in \mathbb{R}^{ExH}$ are all parametrized by the neural network. We then apply an *argmax* function to \mathcal{X}_{prob} to generate the next

word in the sentence. This process is repeated for all words in the sentence.

3.2 Attention Regularization

When weights of the attention mechanism are not regularized, there is a possibility that the network will assign each data point equal attention weights. To this end, we apply a set of regularizations on the attention weights to enforce the network not to choose all the data as its base in making the decision.

Xu's et al. – We first apply the regularization proposed by Xu *et al.* [17] to ensure that all the attention weights sum to one for both temporal direction and spatial direction for local image features extraction. More specifically, Xu *et al.* encourage a doubly stochastic property on the attention matrix which contains attention weights for local image feature extraction at each time step. The loss function for Xu *et al.* is defined as:

$$C_{xu} = \sum_i^N \left(1 - \sum_t^C \alpha_{ti} \right)^2 \quad (3)$$

Salient Alpha (SAL) – The aim for SAL regularization is to increase the distance between the maximum weight and the average weight to force the network to be highly selective when attending to image regions. We define SAL as follows.

$$C_{SAL} = \frac{1}{C} \sum_{t=0}^C \left(\frac{\max_i(\alpha_{ti}) - \text{mean}_i(\alpha_{ti})}{\text{mean}_i(\alpha_{ti})} \right) \quad (4)$$

Where \max_i is the maximum value and mean_i is the mean along the column axis.

Time Distributed Variance (TDVAR) – The TDVAR aims to increase the variance of the attention weights. This will enforce the network to assign different attention weights for each generated word and enforces high variability in the attended features when generating the text sequence. We define TDVAR as follows:

$$C_{TD} = \frac{1}{N} \sum_{i=0}^N \left(\frac{\text{std}_t(\alpha_{ti})}{\text{mean}_t(\alpha_{ti})} \right) \quad (5)$$

Where std_t is the standard deviation and mean_t is the mean along the row axis of α_{ti} . We then combine these three regularization terms to produce C_{alpha} as follows:

$$C_{alpha} = \lambda_1 C_{xu} + \frac{\lambda_2}{\max(\delta, C_{SAL})} + \frac{\lambda_3}{\max(\delta, C_{TD})} \quad (6)$$

where λ_1 , λ_2 and λ_3 are hyperparameters to scale the representation of each term. δ is used to avoid zero division and exploding gradients in the initial training steps.

Table 1: This table provides the quantitative evaluations metrics for the machine generated texts.

Architecture	BLEU-1	BLEU-2	BLEU-3	BLEU-4	ROUGE	METEOR
CORAL8	0.49	0.35	0.28	0.23	0.39	0.31
Recurrent Attention [18]	0.36	0.26	0.21	0.17	0.30	0.29
Xu <i>et al.</i> [17]	0.44	0.30	0.23	0.19	0.35	0.30
VANNILA	0.31	0.19	0.12	0.07	0.30	0.29
CORAL8 w/o clinical notes	0.44	0.29	0.22	0.17	0.34	0.29
CORAL8 w/o TDVAR	0.42	0.22	0.17	0.17	0.37	0.26
CORAL8 w/o Xu’s regularization	0.42	0.30	0.23	0.19	0.36	0.29
CORAL8 w/o SAL	0.41	0.29	0.22	0.18	0.36	0.29
CORAL8 w/o attention regularization	0.44	0.31	0.25	0.20	0.37	0.28

3.3 Training protocol

We use random initialisation for neural network weights and zero initialisation for biases. The embedding matrix $\mathbb{R}^{V \times E}$ is randomly initialised with values between -1 and $+1$. During training, the input to the network is $\mathcal{D}_t = \{\mathcal{I}, \mathcal{R}, \mathcal{Q}\}_i^{D_t} = 0$. The cost function used to train the network is as follows;

$$\text{Cost} = -\log(P(\mathcal{R}|\mathcal{I} \cap \mathcal{Q})) + C_{alpha} \quad (7)$$

We update the gradients of the network using truncated backpropagation through time (TBTT) with $\tau = 2m$ [12] and ADAM optimisation [9] *e.g.* The error is computed over the generated sentence, and the prior encoded previous sentence of lengths m . We implement the norm clipping strategy of [15] to stabilize the network and prevent exploding gradients. During inference, the inputs to the network are $\mathcal{D}_{in} = \{\mathcal{I}, \mathcal{Q}\}_{i=0}^{D_{in}}$. **NEWLINE** tokens serve as the initial word inputs to the sentence generator; which generates the sentence word by word. Sentences are then generated one by one until the entire medical report sequence is complete.

4 Experiments and Results

We prepare the dataset by resizing all images to 224x224x3 pixels in order to make use of a VGG-16 network pre-trained on ImageNet [3]. All words from the medical reports and clinical notes are tokenized and we replace any word that occurs less than two times in the dataset with a special **UNK** token. This creates the vocabulary of 596 words. **NEWLINE** and **EOS** tokens are added to every sentence to indicate the start and end of the sentence respectively. Each sentence is padded to a fixed length of 40 word with **NULL** tokens. Finally, each medical report is padded to a fixed length of seven sentences.

We trained our model for 30 epochs using a learning rate of 0.001, $\lambda_1 = 1$, $\lambda_2 = 0.5$, $\lambda_3 = 0.5$ and $\delta = 0.001$. Then, the performance was evaluated using BLEU [13], ROUGE [11], and METEOR [2]. We use an implementation of [18] to serve as the baseline for our experiment; using the set of eight RDIF images as input instead of the pair of radiology images. We refer to this method as **Recurrent Attention**. The alpha regularization method proposed in [17] applied to our CORAL8 model is also compared as a baseline. We conduct ablation studies to evaluate the contributions of each

Table 2: This table contains abridged examples of machine generated reports. Due to space constraints, we only include the final sentence of the report as it contains the overall impressions. Unabridged examples are included in the supplementary materials. Key words are highlighted red

	Example 1	Example 2	Example 3
Clinical Notes	Renal biopsy. For IF and histology. Creatinine 250. Proteinuria, haematuria, suspected IgA nephropathy	histopathology, IF. Renal failure. Urine protein -/blood positive. ANCA positive. ?ANCA vasculitis. ? Crescentic necrotising GN	Renal Bx. Diabetic. Hypertensive. eGFR 23. Proteinuria.
Ground Truth	iga UNK oxford classification s1 t2 UNK and UNK are UNK due to UNK tissue UNK	pauci immune anca related focal segmental necrotising glomerulonephritis	arterionephrosclerosis with UNK UNK interstitial fibrosis and hypertensive vascular disease glomerulomegaly consistent with grade 1 diabetic glomerulopathy widespread low grade tubular epithelial injury with some atn
CORAL8 with clinical notes	iga nephropathy oxford classification m0 t0	focal segmental necrotising and crescentic pauci immune glomeruli nephritis	acute on chronic thrombotic microangiopathy tma UNK a history of UNK hypertension
CORAL8 without clinical notes	fsgs	there is equivocal reactivity for igg igm c3 and c1q of the glomeruli with a similar intensity.	there is no.

proposed component to the overall performance of our model. To determine the significance of clinical note features, we train a model that omits the initial prior encoder step and uses F_{init} to represent the context vector for the first sentence i.e. $F_0 = F_{init}$. Examples of generated reports with and without clinical notes can be found in Table. 2 To asses the effects of each alpha regularization term; we train a model that omits it from the cost function. We also include a vanilla implementation where the sentence generator consists of LSTM conditioned only on S_t and F_{init} . The quantitative results for all models are provided in Table 1.

5 Discussion and future direction

Table 1 shows that removing any component of the alpha regulation term will result in decreased performance. This suggests that the introduced SAL, TDVAR and clinical notes all contribute to the final performance. Insights into how the clinical notes may be improving results can be inferred from Table 2.

The first example refers to a case of IgA nephropathy; oxford classification S1 T1. S1 indicates that some glomeruli are segmentally sclerosed; this is both a feature of IgA nephropathy and focal segmental glomerular sclerosis (FSGS). The model without clinical notes concluded the image was FSGS, but the presence of *suspected IgA nephropathy* in the clinical notes resulted in the proposed model predicting IgA nephropathy in the generated report. In the second example, the proposed model accurately predicts pauci immune glomeruli nephritis. This condition is often referred to as Anti-neutrophil cytoplasmic antibody (ANCA) associated vasculitis, due to its strong association with ANCA antibodies [7]. The presence of *ANCA positive ?ANCA vasculitis*

in the clinical notes suggests that the proposed model is capturing the associations between the clinical context and the pathologist impressions of the RDIF assay. Example 3 in Table 2 illustrates an incorrect impression generated by the CORAL8 model. Despite being incorrect, the example illustrates how conditions with similar clinical features are modelled by the network. The underlying pathophysiology for both the ground truth condition (arterionephrosclerosis) and the predicted condition (thrombotic microangiopathy) can be due to the clinically observed hypertension [8, 10]. This suggests that the distributions are similar for pathologies that present with shared clinical features; indicating a degree of semantic understanding.

6 Acknowledgements

This project has been funded by Sullivan Nicolaides Pathology and the Australian Research Council (ARC) Linkage Project [Grant number LP160101797].

References

- [1] Alsaad, K., Herzenberg, A.: Distinguishing diabetic nephropathy from other causes of glomerulosclerosis: an update. *Journal of clinical pathology* 60(1), 18–26 (2007)
- [2] Banerjee, S., Lavie, A.: Meteor: An automatic metric for mt evaluation with improved correlation with human judgments. In: *Proceedings of the acl workshop on intrinsic and extrinsic evaluation measures for machine translation and/or summarization*. pp. 65–72 (2005)
- [3] Deng, J., Dong, W., Socher, R., Li, L.J., Li, K., Fei-Fei, L.: Imagenet: A large-scale hierarchical image database. In: *CVPR*. pp. 248–255. Ieee (2009)
- [4] Donahue, J., Anne Hendricks, L., Guadarrama, S., Rohrbach, M., Venugopalan, S., Saenko, K., Darrell, T.: Long-term recurrent convolutional networks for visual recognition and description. In: *CVPR*. pp. 2625–2634 (2015)
- [5] Graves, A., Schmidhuber, J.: Framewise phoneme classification with bidirectional lstm and other neural network architectures. *Neural Networks* 18(5-6), 602–610 (2005)
- [6] Ho, J., Ahlers, S.M., Stratman, C., Aridor, O., Pantanowitz, L., Fine, J.L., Kuzmishin, J.A., Montalto, M.C., Parwani, A.V.: Can digital pathology result in cost savings? a financial projection for digital pathology implementation at a large integrated health care organization. *Journal of pathology informatics* 5 (2014)
- [7] Kallenberg, C.G., Heeringa, P., Stegeman, C.A.: Mechanisms of disease: pathogenesis and treatment of anca-associated vasculitides. *Nature Reviews Rheumatology* 2(12), 661 (2006)
- [8] Khanal, N., Dahal, S., Upadhyay, S., Bhatt, V.R., Bierman, P.J.: Differentiating malignant hypertension-induced thrombotic microangiopathy from thrombotic thrombocytopenic purpura. *Therapeutic advances in hematatology* 6(3), 97–102 (2015)
- [9] Kingma, D.P., Ba, J.: Adam: A method for stochastic optimization. *arXiv preprint arXiv:1412.6980* (2014)

- [10] Kopp, J.B.: Rethinking hypertensive kidney disease: arterionephrosclerosis as a genetic, metabolic, and inflammatory disorder. *Current opinion in nephrology and hypertension* 22(3), 266 (2013)
- [11] Lin, C.Y.: Rouge: A package for automatic evaluation of summaries. *Text Summarization Branches Out* (2004)
- [12] Mikolov, T., Karafiat, M., Burget, L., Černocky, J., Khudanpur, S.: Recurrent neural network based language model. In: Eleventh annual conference of the international speech communication association (2010)
- [13] Papineni, K., Roukos, S., Ward, T., Zhu, W.J.: Bleu: a method for automatic evaluation of machine translation. In: Proceedings of the 40th annual meeting on association for computational linguistics. pp. 311–318 (2002)
- [14] Pascanu, R., Gulcehre, C., Cho, K., Bengio, Y.: How to construct deep recurrent neural networks. arXiv preprint arXiv:1312.6026 (2013)
- [15] Pascanu, R., Mikolov, T., Bengio, Y.: On the difficulty of training recurrent neural networks. In: ICML. pp. 1310–1318 (2013)
- [16] Simonyan, K., Zisserman, A.: Very deep convolutional networks for large-scale image recognition. arXiv preprint arXiv:1409.1556 (2014)
- [17] Xu, K., Ba, J., Kiros, R., Cho, K., Courville, A., Salakhudinov, R., Zemel, R., Bengio, Y.: Show, attend and tell: Neural image caption generation with visual attention. In: ICML. pp. 2048–2057 (2015)
- [18] Xue, Y., Xu, T., Long, L.R., Xue, Z., Antani, S., Thoma, G.R., Huang, X.: Multimodal recurrent model with attention for automated radiology report generation. In: MICCAI. pp. 457–466. Springer (2018)
- [19] Zhang, Z., Xie, Y., Xing, F., McGough, M., Yang, L.: Mdnet: A semantically and visually interpretable medical image diagnosis network. In: CVPR. pp. 6428–6436 (2017)